Lab on a Chip

Cite this: *Lab Chip*, 2012, **12**, 4296–4304

www.rsc.org/loc

PAPER

Seed particle-enabled acoustic trapping of bacteria and nanoparticles in continuous flow systems†

Björn Hammarström,*[a] Thomas Laurell[ab] and Johan Nilsson[a]

Received 20th June 2012, Accepted 6th August 2012
DOI: 10.1039/c2lc40697g

Acoustic trapping of sub-micron particles can allow enrichment and purification of small-sized and low-abundance microorganisms. In this paper, we investigate the dependency of the ability to capture sub-micron particles on the particle concentration. Based on the findings, it is demonstrated that seed particles can be introduced to acoustic trapping, to enable capture of low-abundance sub-micron particles. Without using seed particles, continuous enrichment of 490 nm polystyrene particles is demonstrated in a rectangular capillary with a locally generated acoustic field at high particle concentrations, *i.e.* above 1% wt. Trapping of sub-micron particles at significantly lower concentrations was subsequently accomplished by seeding 10–12 micrometer-sized particles in the acoustic trap prior to the sub-micron particle capture. Furthermore, the new seeded-particle-aided acoustic trapping technique was employed for the continuous enrichment of bacteria (*E. coli*) with a capture efficiency of 95%. Finally, seed particle assisted acoustic trapping and enrichment is demonstrated for polymer-based particles down to 110 nm in diameter.

Introduction

Retention and trapping of particles in microfluidic systems is a key unit operation in the development of systems for advanced cell and particle handling. A wide range of both mechanical traps as well as non-contact trapping techniques have been reported.[1] Microfluidic systems designed for non-contact trapping are usually less prone to clogging when analyzing crude biological samples and many times the absence of surface interaction yields less perturbed cell populations in a subsequent study. Non-contact trapping is accomplished by imposing a force field, which can retain particles against viscous drag. The imposed field may be of electrical,[2] optical,[3] hydrodynamic[4] or acoustic[1] origin.

In line with the development of more advanced microfluidic cell handling systems, techniques that enable trapping of biological components of sub-micrometer dimensions are in high demand. This may be bacteria, sub-cellular organelles, or even viral particles. Trapping and enrichment of single micron- or sub-micron sized particles have high-impact applications in sample preparation for bioanalytics or diagnostics, be that in clinical (*e.g.* sepsis, chlamydia), environmental (*e.g.* water and food stuff control) or forensic analysis (*e.g.* biowarfare or sexual assault). The ability to trap particles in a non-contact mode against flow inherently enables enrichment of a rare species and hence improved system detection limit. Also, non-contact trapping systems offer means to analyze or study the trapped species after enrichment and washing, as they undergo sequential chemical assays, *e.g.* in terms of biospecific analysis protocols or in terms of drug interaction studies.

In microfluidic systems both optical tweezers and dielectrophoretic (DEP) trapping allow capture of sub-micron particles. In 1987 Ashkin and Dziedzic showed the possibility to use optical tweezers for capture of viruses and bacteria.[5] In DEP the use of high-resolution microfabricated electrodes allowed sufficiently high electric field gradients to overcome the negative volume scaling of the particle forces for particles down to 100 nm scale.[6] Later chip integrated insulator dielectrophoresis was demonstrated in an array of insulating posts, concentrating and separating live and dead *E. coli*.[7] However, for applications in sample preparation (*i.e.* enrichment or washing) the practical usefulness of these techniques has been limited by relatively low sample processing rates.

Acoustic trapping has emerged as a useful tool for handling eukaryotic cells in biological assays[8,9] and in contrast to optical tweezers and DEP-trapping allows handing of larger number of cells at high flow rates.[1] Manipulation and concentration of sub-micron particles and microorganisms in stationary liquid batch systems have *e.g.* been demonstrated by Sobanski *et al.*,[10] Limaye *et al.*[11] and Kuznetsova.[12] The ability to handle a large number of cells with retained viability[13,14] in combination with relatively high volumetric flow rates make acoustic methods well suited for sample enrichment and preprocessing. This was recently demonstrated by Norris *et al.*, using acoustic trapping

[a]*Department of Measurement Technology and Industrial Electrical Engineering, Lund University, Sweden.*
E-mail: Bjorn.Hammarstrom@elmat.lth.se; Fax: +46462224527; Tel: +46462229371
[b]*Department of Biomedical Engineering, Dongguk University, Seoul, Korea*
† Electronic supplementary information (ESI) available. See DOI: 10.1039/c2lc40697g

to automate enrichment and washing of sperm cells for forensic analysis in sexual assault cases.[15]

Acoustic trapping systems, designed as local acoustic resonators can allow efficient particle trapping in low complexity microfluidic devices. To enable acoustic trapping within a microfluidic system, the acoustic energy has to be localized to a specific trapping area. This concept has been demonstrated in two device types, either by using a resonating cavity[16] or by using a localized actuation.[17,18] We recently demonstrated that the concept of localized actuation combined with disposable rectangular cross-section capillaries (acting as ultrasonic resonators) provided a low complexity and low cost disposable system with good performance in terms of operating flow rate and induced trapping force.[19]

The major challenge when applying acoustic standing wave technology for sub-micron particle manipulation is the scaling laws of the primary acoustic particle forces and the hydrodynamic drag force resulting from the induced acoustic streaming. As particles get smaller a rapid decrease in primary acoustic particle force in relation to Stokes drag occurs. The particle size region where a transition to a drag dominated behavior occurs is a system specific parameter that typically is found around a single micron for aqueous based systems operated in the range of 2 MHz.[20] In contrast to techniques such as DEP, the induced acoustic streaming is significant and capture cannot be realized by simply decreasing the sample flow rate.

In this work we show that the ability to acoustically trap sub-micrometer particles against a flow is dependent on the particle concentration, and that particle–particle interactions play an important role in this process. These results are used to elucidate the idea of pre-loading larger seed particles in the acoustic trap to enhance sub-micron particle capture.[21] Furthermore, the ability to initiate clustering of 110 nm particles is shown, and enrichment of low concentration bacteria (*E. coli*) in continuously flowing suspensions is reported in terms of capture efficiency and throughput.

Theory

As a basis for discussion of acoustic sub-micron particle capture, a brief review of the theory behind acoustic trapping is provided, Fig. 1. This description is largely based on Woodside *et al.*[22] that provides a comprehensive description of the mechanisms for capture and aggregation based on original papers from Gorkov,[23] Whitworth *et al.*,[24] Crum[25] and Weiser.[26]

Primary forces

Primary radiation forces (PRF) are exerted directly on the particles by the incident acoustic wave. When considering the case of a plane standing acoustic wave, an expression for the axial PRF on a spherical particle (with a radius much smaller than the wavelength) can be derived.[22]

$$F_{\mathrm{Axi}} = -V_{\mathrm{p}} \cdot E_{\mathrm{ac}} \cdot k \cdot \Phi \cdot \sin(2kx)$$

$$\Phi = \left(\frac{3(\rho_p - \rho_m)}{\rho_m + 2\rho_p} + \frac{\beta_m - \beta_p}{\beta_m} \right) \quad (1)$$

Here, V_{p} is the volume of the particle, E_{ac} is the acoustic energy density, k is the wavenumber, β is compressibility and ρ is density where m denotes the media and p denotes the particle. The Φ factor in eqn (1) (based on density and compressibility of particles in relation to the media) determines the direction of the primary radiation force. For cells or bacteria in an aqueous suspension this factor is typically positive, such that the axial PRF will be directed towards the pressure nodes of the standing wave. In the context of the trapping device based on rectangular cross-section capillaries (Fig. 2) used in this work, the axial PRF can be used to understand both particle levitation and the formation of thin particle layers.[19]

The lateral PRF can explain particle retention in a system where the fluidic flow is aligned orthogonal to the standing wave. In real geometries, 3D localization of the standing wave will create gradients in the acoustic energy density that are perpendicular to the standing wave. The lateral PRF can be expressed as a function of these gradients.[22]

$$F_{\mathrm{Lat}} = V_{\mathrm{p}} \nabla E_{\mathrm{ac}} \left(\frac{3(\rho_p - \rho_m)}{\rho_m + 2\rho_p} \cos^2(kx) - \frac{\beta_m - \beta_p}{\beta_m} \sin^2(kx) \right) \quad (2)$$

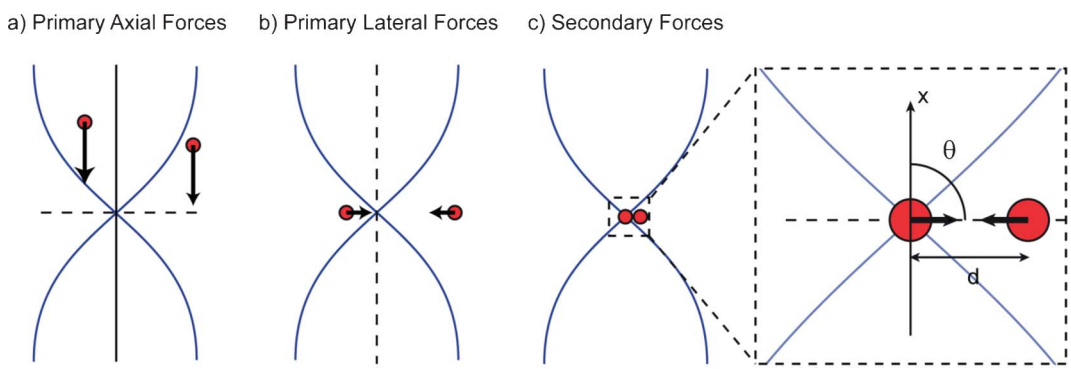

Fig. 1 The mechanisms of particle capture and aggregation in an acoustic trap can be described in three steps: (a) Primary axial radiation forces move particles to the nodal plane of a standing wave allowing particle levitation; (b) The 3D gradient of the acoustic field also creates lateral radiation forces that retain the particles in the trap; (c) The secondary acoustic forces become significant and cause aggregation, when particle to particle distances are small.

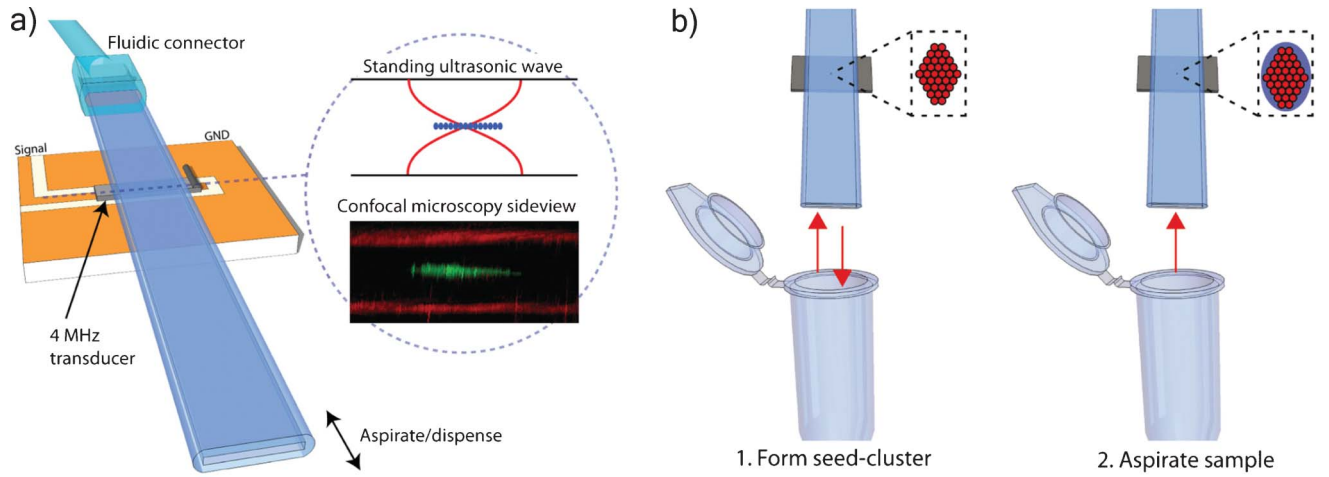

Fig. 2 (a) An overview of the capillary-based system for non-contact acoustic trapping. A miniaturized 4 MHz piezoelectric transducer locally actuates the cross-sectional resonance of 0.2 × 2 mm capillary. Particles were trapped in non-contact mode above a miniaturized transducer in the pressure node of the standing acoustic wave. Confocal microscopy confirmed that the beads (green fluorescence) were levitated in the center of the channel (red reflections from water–glass interface). (b) Seed particles were aspirated and trapped, forming a thin layer (1) and the sample containing *E. coli* was subsequently aspirated and trapped (2).

This means that the lateral radiation forces will direct particles to the local acoustic energy density maxima if they can be regarded as dense and incompressible in relation to the media.

Secondary forces

Secondary acoustic forces become significant at close inter-particle distances. These forces arise from the interaction of acoustic waves scattered from the particles. For two spherical particles of identical radius the secondary acoustic force (F_{Sec}) can be expressed as[27]:

$$F_{Sec} = 4\pi a^6 \left\{ \frac{(\rho_p - \rho_m)^2 (3\cos^2\theta - 1)}{6\rho_m d^4} v^2(x) - \frac{\omega^2 \rho_m (\beta_p - \beta_m)^2}{9d^2} p^2(x) \right\} \quad (3)$$

Here, v is the velocity field, p is the pressure field, ω is the angular frequency, a is the particle radius, d is the inter-particle distance, and θ is the angle between the axis of the incident wave and the centerline connecting the two particles, Fig. 1c.

The secondary force scales with the volume of both particles (radius to the power of six if both particles have the same size, eqn (3)) and the distance between them. There are two terms, one which is dependent on density difference and one which is dependent on compressibility difference. Both of these terms increase in magnitude with closer inter-particle distance but the scaling is different. The compressibility based term is an attractive force that can be expected to be most relevant for intermediate inter-distances whereas the density based term have both an angular dependence and display a stronger scaling with the inter-distance. For this reason the density term might be expected to dominate at very short center–center distances and be the dominating term for very small particles since the double radius limit is lower. The density term displays dependence to the angle between the centerline of the particles and the axis of the incident wave making the force contribution attractive in the plane perpendicular to the direction of the standing wave and repulsive for particles aligned with the standing wave.

Acoustic streaming

The ultrasonic standing wave will also induce fluidic motion in the channel known as acoustic streaming. The origin of the streaming can be effects in the fluidic boundary layers (close to solid wall) or attenuation of ultrasound as it propagates in the media. Acoustic streaming produces recirculating flows that are classified based on the length scale and the mechanisms involved: Eckart streaming[28] produces container scale streaming rolls, Rayleigh streaming[29] produces wavelength scale rolls and Schlichting streaming[30] creates flows within the viscous boundary layer close to the wall.

In small particle capture the acoustic streaming is typically the limiting factor.[20,21] This is due to the scaling of the primary radiation forces and the Stokes drag. The PRF scales with the volume of the particle (eqn (1) and (2)) whereas the Stokes drag scales with the radius of the particle. In a given system that induces a specific streaming velocity and radiation force relative to the particle size there will be a cutoff particle size that determines whether the particle will be retained by the primary forces or lost with the acoustic streaming.

Materials and methods

Experimental setup

It was recently shown that borosilicate glass capillaries with a rectangular cross-section (Vitrotubes, VitroCom, USA) can be used for non-contact acoustic trapping of cells and microparticles when combined with a miniaturized ultrasonic transducer.[19] This setup was applied in this work using a 0.2 × 2 mm (inner dimensions) capillary and a 4 MHz PZT transducer, Fig. 2. Exiting the top–bottom resonance (the shortest distance) of the capillary by a small transducer produces a localized standing ultrasonic wave providing significant lateral forces that can retain particles against flow above the transducer.

A schematic of the assembled device is shown in Fig. 2 where a transducer is mounted on a printed circuit board. The capillary is held in place by a Perspex^{TM} clamp and a thin layer of glycerol is used as coupling medium between the transducer and the capillary. This kind of setup provides the opportunity to dispose capillaries between experiments. The acoustic trapping capillary is operated in aspirate/dispense mode by connecting one end of the capillary to a syringe pump and aspirating the samples *via* the other. This mode of operation provides a versatile system for sample control and allows easy extraction of captured particles with a minimal dead volume when collecting captured particles.

Actuation settings and instrumentation

During all the experiments in this paper the same capillary and transducer was used. Actuation of the ultrasonic transducer was done using a function generator (HP 33120A, Hewlett-Packard, USA) driving the PZT with a sine-wave of 4 MHz at 17 V_{PP} amplitude. These settings were tuned to the resonance of the capillary and the voltage was chosen to provide minimal heating while having sufficient acoustic forces. For fluid control with minimal pulsation a linear motor syringe pump (neMESYS, Cetoni GmbH, Germany) was used.

Concentration dependence in acoustic trapping of small particles and bacteria

The concentration dependence in small particle trapping was evaluated using yellow fluorescent polystyrene beads (Kisker Biotech GmbH & Co. KG, Germany) with diameters 0.490, 1.84 and 3 μm. Phosphate buffered saline (PBS) with 0.05% Triton-X was used as running buffer and for preparing dilution series. Here, the detergent was used to minimize non-acoustically induced agglomeration. Furthermore, aggregation due to intermolecular forces has been shown to produce open dendritic clusters whereas trapping of non-adhering particles results in close packed structures.[31] The formation of densely packed clusters (as visible from the 3 μm particles) was used as a control to verify that the buffer did not cause aggregation.

To isolate the effects of the acoustically induced particle motion the first experiments were done with zero flow. A demonstration of the acoustic streaming in the device and the effects of concentration was done with 490 nm beads at the two concentrations; 0.1 and 1%wt.

An applied flow of 10 μL min^{-1} was used to characterize small particle capture/enrichment at different concentrations. To quantify the trapping over time the total fluorescence intensity in the trapping area was measured once every second using a camera (Orca-R2, Hamamatsu, Japan) connected to the microscope. This was done during a time interval starting a few seconds before transducer activation. A flat intensity line was taken as unsuccessful capture whereas a linear increase was taken as successful capture and collection of fluorescent particles. To investigate the concentration dependence for different bead sizes experiments were done for; 490 nm beads at concentrations 1, 0.75, 0.5, 0.25%wt, 1.84 μm beads at 0.25, 0.125 and 0.0625%wt and 3 μm beads at concentrations 0.0625, 0.03125 0.015625%wt.

Acoustic trapping of small biological species was evaluated using *Escherichia coli* (*E. coli*) strain DH5α as a model. The bacteria were fluorescently stained using a bacterial viability kit (LIVE/DEAD BacLight L7012, Invitrogen, USA) producing a green fluorescence in the viable bacteria. Bacteria concentrations were measured by manual counting in a Bürker chamber.

The concentration limit for *E. coli* capture was established by making 1 : 10 dilutions from 50 × 10^3 bacteria μL^{-1} and measuring fluorescent increase at each concentration. To allow direct comparison to the results from the bead experiments a flow of 10 μL min^{-1} was used.

E. coli capture using seed particles

The possibility to circumvent the concentration limitation by using seed particles was demonstrated at an *E. coli* concentration of 5 × 10^3 bacteria/μL (significantly below the established concentration limit for non seed particle induced trapping) at a flow rate of 10 μL min^{-1}. To initiate clustering and allow capture at lower concentrations 10 μm blue colored polystyrene beads (FLUKA BioChemica 55463, Fluka Chemie AG, Switzerland) were used as seed particles. As shown in Fig. 2b, the aspirate/dispense functionality was used to form a thin layer of seed particles, and subsequently the bacteria solution was aspirated, while capture was monitored by fluorescence. Seed particles of 10 μm diameter were chosen, since previous work has shown the possibility to obtain levitated mono-layers,[19] allowing unobstructed optical feedback from captured particles.

Low concentration *E. coli* capture

Individual capture of *E. coli* was analyzed by monitoring capture efficiency at a concentration of 110 bacteria μL^{-1}. The capture efficiency was measured by manually counting fluorescently labeled *E. coli* in micrographs taken of the channel. With a field of view (FOV) in the microscope corresponding to 0.39 μL (calculated using the capillary depth of 200 μm) the predicted number of bacteria per FOV were 43, such that individual capture events could be resolved in the micrographs. Four cases were studied with ten images each; 1.5 mm upstream from the acoustic trap with seeding, 1.5 mm downstream from the acoustic trap with seeding, without seeding, and without an active ultrasonic transducer.

To characterize the throughput of the system a study of the capture rate at higher flow-rates was performed. Using an *E. coli* concentration of 50 bacteria μL^{-1} the fluorescence increase was evaluated for three different flow rates: 10 μL min^{-1}, 30 μL min^{-1} and 90 μL min^{-1}. To minimize the auto-fluorescence from the seed cluster (generated by the blue color of previously used beads), 12 μm plain (non-colored) polystyrene beads (Fluka Chemie AG, Switzerland) were used as seed particles during all the low concentration experiments.

Nanoparticle capture

To demonstrate the ability to apply seed particle trapping to nanoparticles, capture of 110 nm particles was evaluated. Red fluorescent polystyrene beads (Kisker biotech) with a diameter of 110 nm were used as the target particles and seeding was done with 10 μm polystyrene beads (Fluka, BioChemica 55463). A thin layer of 10 μm beads was trapped and subsequently a solution of 110 nm beads at a concentration of 0.1%wt was aspirated at a flow rate of 10 μL min^{-1}. By monitoring the

increase of nanoparticle specific fluorescence on the trapped cluster capture of the 110 nm beads could be evaluated and for comparison images where taken using the autofluorescence of the seed particles. Reference experiments with direct capture of the 110 nm particles at the same flow rate were evaluated for concentrations up to 1%wt.

Results and discussion

Concentration dependence in acoustic trapping of small particles

The acoustic streaming pattern in the trapping capillary with no external flow applied is shown in Fig. 3a using 490 nm fluorescent beads at a concentration of 0.1%wt. When actuated at resonance, this device produced four characteristic streaming rolls generating recirculation flows with a radius defined by the edge of the transducer and the width of the capillary. The orientation of the streaming rolls was such that particles were moved inwards towards the trapping area along the extension axis of the capillary and moved outwards towards the walls of the capillary above the transducer. Similar streaming patterns have been reported by and applied for mixing purposes.[32] It should be noted that no trapping/aggregation of the particles occurs at this concentration level.

A transition from streaming to trapping behavior was observed when increasing the concentration of 490 nm beads from 0.1%wt to 1%wt, Fig. 3b. The trapped cluster of 490 nm beads was continuously growing as particles were translated to the trapping site by acoustic streaming.

Applying an external flow (10 μL min^{-1}) showed the possibility to perform capture/enrichment of 490 nm particles as the particle concentration was elevated, Fig. 4a. Measuring the total fluorescence intensity in the trapping area clearly showed successful enrichment at 1%wt in form of a linear increase in fluorescence intensity. Decreasing the concentration in steps of 0.25%wt showed that the transition from trapping to streaming occurred between 0.75 and 1%wt for the 490 nm particles. At elevated concentrations capturing was initiated instantaneously after transducer activation (at 5 s in Fig. 4a) whereas after a 25% decrease in concentration capturing could not be observed in our experiments. This supports that a transition from a trapping to a streaming dominated regime occurs between these concentrations.

The transition from trapping to streaming was evaluated for three different bead sizes, Fig. 4b, by taking the lowest found concentration that produced an increase in fluorescence intensity as the concentration limit for successful trapping. Under these conditions a trapping and a streaming regime can be identified for different bead sizes. It was found that substantially increased concentrations were required to capture the smaller particles.

The data shows that it is in fact possible to trap and enrich sub-micron particles below the streaming limit if the particle concentration is sufficiently high. These results are in agreement with previous reports from Miles *et al.*[33] that indicate a similar influence of concentration for stationary flow manipulation of micro-organisms. The mechanisms causing aggregation at high concentration may be related to a combination of hydrodynamic interaction[34] and secondary acoustic radiation forces. The secondary acoustic force (eqn (3)) scales with the inter-particle distance and the particle volumes. Since an increase in concentration will correspond to a decrease in the inter-particle distance the influence of secondary forces will become more important at elevated concentrations. At sufficiently short inter-particle distances aggregation by secondary acoustic forces might occur, potentially triggering a cluster formation. Once a larger particle aggregate is formed the primary acoustic forces may retain this against fluid flow. Note here, that the effects responsible for aggregation may occur in a way such that they are not in competition with fluidic drag. Above the transition particle-concentration the average inter-particle distance may be sufficiently short as to trigger these effects instantaneously whereas below the transition there is a rapidly decreasing chance of aggregation.

The ability to apply the concentration dependence of acoustic trapping to capture and enrich small biological species was tested using *E. coli* as a model. Enrichment was evaluated by measuring the fluorescence intensity increase in the trap under continuous inflow of fluorescently labeled *E. coli* at a flow rate of 10 μl min^{-1}. Indeed, a transition from trapping to streaming behavior was established between 50 × 10^3 bacteria μL^{-1} and 5 × 10^3 bacteria μL^{-1}, Fig. 5. At 50 × 10^3 bacteria μL^{-1} a

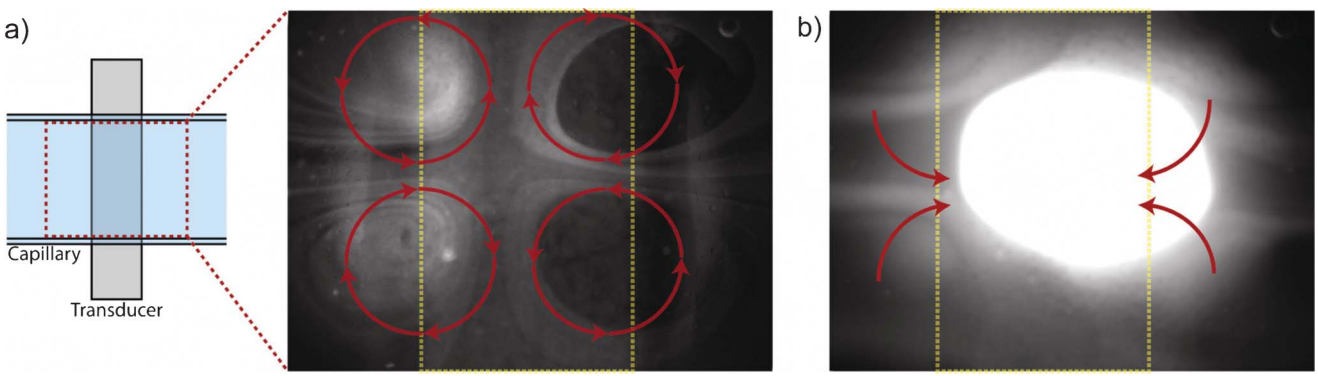

Fig. 3 (a) The acoustic streaming pattern in the trapping capillary is shown using 490 nm particles at a concentration of 0.1%wt. The capillary is horizontally aligned and the transducer is outlined in yellow. Four characteristic streaming rolls are observed for this setup at resonance as indicated by the red arrow (supplemental: video 1 streaming rolls). (b) Increasing the concentration of 490 nm particles from 0.1%wt to 1%wt triggers aggregation of the sub-micron particles. Outside of the transducer area the particles are still affected by streaming and translated to the trapping zone such that the size of the cluster increases over time (supplemental: video 2 hc aggregation).

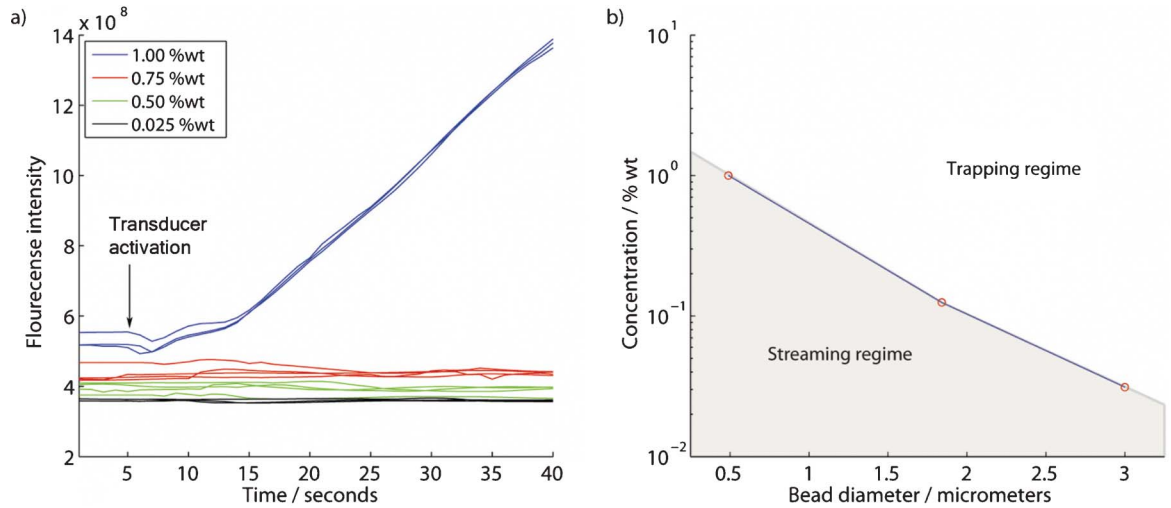

Fig. 4 (a) Successful capture/enrichment of 490 nm particles occurs at high concentrations using an externally applied flow of 10 μL min^{-1} (each trace corresponds to a separate experiment). (b) The lowest concentration for successful enrichment found using sequential ×2 dilutions is plotted against bead diameter.

linear increase of fluorescent signal was observed showing a continuous enrichment of the bacteria whereas at ×10 dilution no trapping occurred as is seen by the absence of fluorescent increase. It can be concluded that the *E. coli* shows principally the same behavior as the 490 nm beads and that the transition between capture and enrichment in our system occurs above 5 × 10^3 bacteria μL^{-1} at a flow rate of 10 μL min^{-1}.

Bacteria capture using seed particles

The acoustic trap was pre-loaded with a small cluster of larger particles (seed particles), that were easily retained against flow. This provided particles that immediately could generate inter-particle forces *versus* the sub-micron particles in the subsequently aspirated sample. The seed particles thereby enabled acoustic trapping and enrichment of *E. coli* below the concentration limit, Fig. 6. Trapping a thin layer of 10 μm beads prior to aspirating

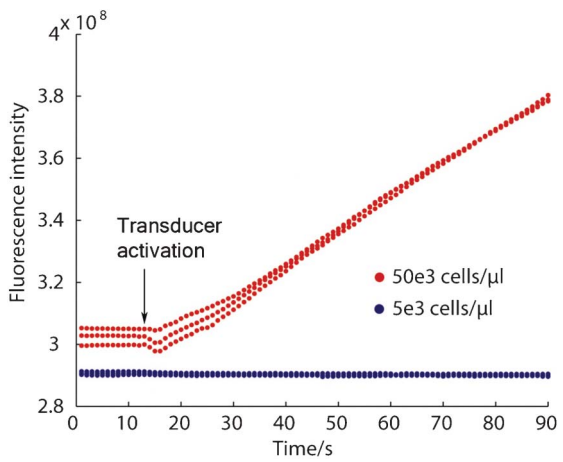

Fig. 5 Enrichment of *E. coli* is possible at elevated concentrations (red traces) while at lower concentrations no trapping occurs (blue traces). A transition from trapping to streaming behavior is observed when decreasing the concentration, analogous to the concentration dependence that was shown with the polystyrene beads.

E. coli at 5 × 10^3 bacteria μL^{-1} with 10 μL min^{-1} allowed capture at the sub-critical *E. coli* concentration, shown by the increasing fluorescent signal.

As hypothesized, large particle–small particle interaction could be used to trigger the effects of inter-particle forces observed at elevated sub micrometer particle concentrations. The insert micrographs in Fig. 6 show a time laps sequence of the bacteria trapping. Initially the bacteria were captured in-between the 10 μm particles (100 s), as the cluster grew the bacteria and the seed particles competed for the central positions in the trap, and finally the bacteria formed a cluster that disrupted the densely packed seed particle layer (300 s and 900 s). This process was monitored over the course of 30 min and showed the possibility to achieve high enrichment factors, as the sample can be passed over the trapping region repeated times and is only limited by the trapping capacity of the system. In conclusion, these results demonstrate that the seed particle strategy enables enrichment of bacteria at levels well below the critical bacterial density.

Low concentration bacteria capture

A reduced concentration (110 bacteria μL^{-1}) allowed *E. coli* to be monitored individually by fluorescence imaging during capture. The capture efficiency of *E. coli* was evaluated by manual counting of fluorescent bacteria in the channel upstream and downstream in relation to the seed cluster, Table 1. This was done at a flow of 10 μL min^{-1} with images taken 1.5 mm from the trapping site. Comparison between the bacteria count upstream and downstream from the cluster resulted in a capture efficiency of 95 ± 3%.

The analysis method for capture efficiency was based on maintaining a constant inflow of bacteria during the experiment. Two reference cases were analyzed to validate this assumption (Table 1); active transducer without seeding resulting in 43 ± 4 bacteria, and inactive transducer resulting in 45 ± 5 bacteria. Based on the sample concentration and the volume under the FOV the expected bacteria count was 43. While there might

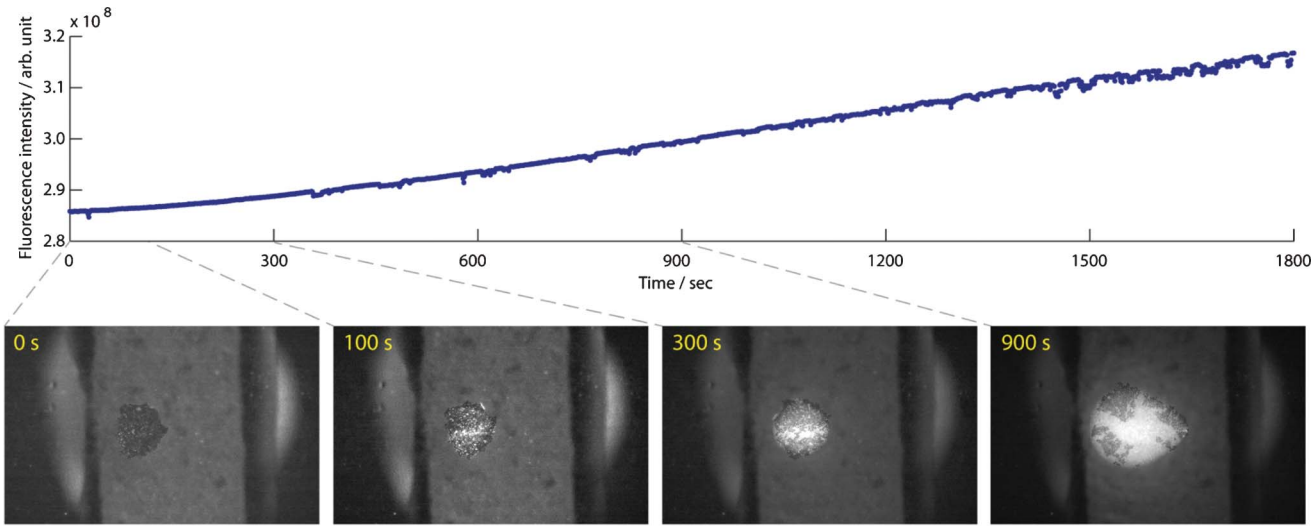

Fig. 6 Trapped seed particles allow capture and enrichment of *E. coli* at a sub-critical concentration for this system (5×10^3 bacteria μL^{-1}). Enrichment of *E. coli* at 10 $\mu L\ min^{-1}$ over the course of 30 min shows the high trapping capacity of the system, and the insets provide visualization of the process at selected time points .

Table 1 A capture efficiency of 95 ± 3% was measured for *E. coli* at 10 $\mu L\ min^{-1}$, based on manual counting of bacteria 1.5 mm upstream and downstream relative to the trapping site

Location:	Upstream	Downstream, with seeding	Downstream, without seeding	Downstream, without active trap
Bacteria count:	39 ± 4	2 ± 1	43 ± 4	45 ± 5

indeed be some variation in the inflow of bacteria, considering the standard deviations of the measurement the results are close to the expected value.

Low-abundance bacteria-trapping was also performed in continuous flow, demonstrating long-term enrichment. Fig. 7 shows the fluorescence increase during *E. coli* enrichment with a sample concentration of 50 bacteria μL^{-1} the flow rates: 10 $\mu l\ min^{-1}$, 30 $\mu l\ min^{-1}$ and 90 $\mu l\ min^{-1}$. A linear increase in fluorescence intensity was observed at all three flow rates. At this concentration the bacteria-bacteria spacing is sufficiently large for the bacteria to be captured as single events, showing that the trapping is independent of the target-species concentration in the sample. Seed particle induced acoustic trapping thereby facilitates enrichment and purification of sub-micron species in highly dilute samples. For optimal performance capture efficiency and sample throughput still has to be matched.

Further insight on optimizing the sample throughput (*i.e.* capture rate) can be gained from analyzing the slopes of the fluorescence increase in Fig. 7, as recorded for flow rates of 10, 30 and 90 $\mu L\ min^{-1}$. At 10 $\mu L\ min^{-1}$ the capture efficiency is 95%, Table 1. When increasing the flow from 10 $\mu L\ min^{-1}$ to 30 $\mu L\ min^{-1}$ the slope in the fluorescence recording increases from 0.059 to 0.12, *i.e.* a factor 2.1 which if the capture efficiency was unaffected by flow rate should have been a factor of 3. This indicates a reduction in capture efficiency to 65%. When further increasing the flow rate to 90 $\mu L\ min^{-1}$ the slope shows a capture efficiency of 61%. The results given in Table 2 suggest that operating at higher flow rates may be beneficial in applications where the major challenge is a low concentration in a large sample volume and throughput is the major priority. If the application on the other hand is purification of sub-micron species in a rare/expensive sample a low flow rate should be chosen to maximize the capture efficiency.

Table 2 Calculated capture efficiencies at elevated flow rates by analysis of the rate of fluorescence increase (slope) in Fig. 7

Flow rate ($\mu L\ min^{-1}$):	10	30	90
Slope [arb. unit/s]:	0.059	0.121	0.34
Capture efficiency:	95% (table1)	65%	61%

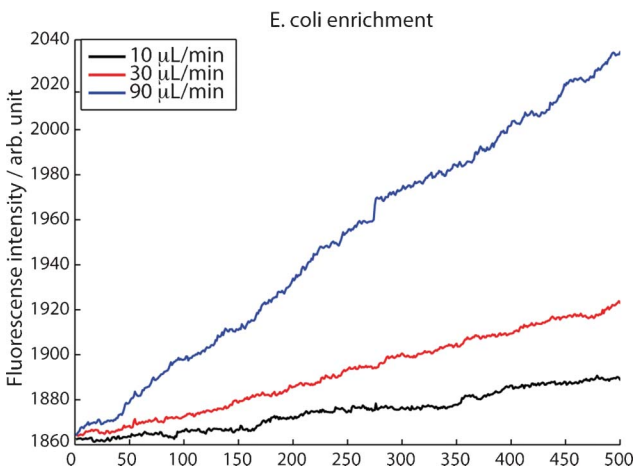

Fig. 7 Capture rate of individually captured *E. coli* (50 bacteria μL^{-1}) at three different flow rates, an increased capture rate is observed at increased flow rates.

In contrast to other acoustophoretic manipulation techniques,[35] seed particle aided acoustic trapping enables trapping below the streaming limitation without reduced performance. This allows for applications such as enrichment and purification/washing of sub-micron species to be carried out in a disposable device.

Although acoustic streaming inherently counteracts acoustic trapping of sub-micron species, the introduction of seed particles to promote trapping may benefit from the streaming. The circular streaming pattern in the system (Fig. 3a) brings the small particles from a wide channel area in close proximity to the seed particles promoting trapping, as can be seen in ESI movie S1†. It is therefore possible that the capture efficiency is not only dependent of the sample flow rate but is also related to the magnitude of the rotational flow. These experiments indicate that the capture efficiency is highly dependent on delivery of the target particle to the seed cluster whereas once captured the inter-particle forces seem sufficient to retain in the trapping site even at highly elevated flows (linear increase at all flows in Fig. 7). A maximum capture rate is reached either by loss of the seed cluster itself or by an unacceptable decrease in capture efficiency.

Nanoparticle capture

The seed particle strategy extends into nanometer size particles, and for the first time acoustic trapping of particles in the 100 nm regime was accomplished. Fig. 8 shows capture of 110 nm red fluorescent particles using 10 μm seed particles. Trapping of the nanoparticles was confirmed using the red fluorescence in contrast to the green autofluorescence of the seed particles. The nanoparticles were captured at a concentration of 0.1%wt whereas reference experiments with direct capture showed that capture was not possible even at a concentration of 1%wt.

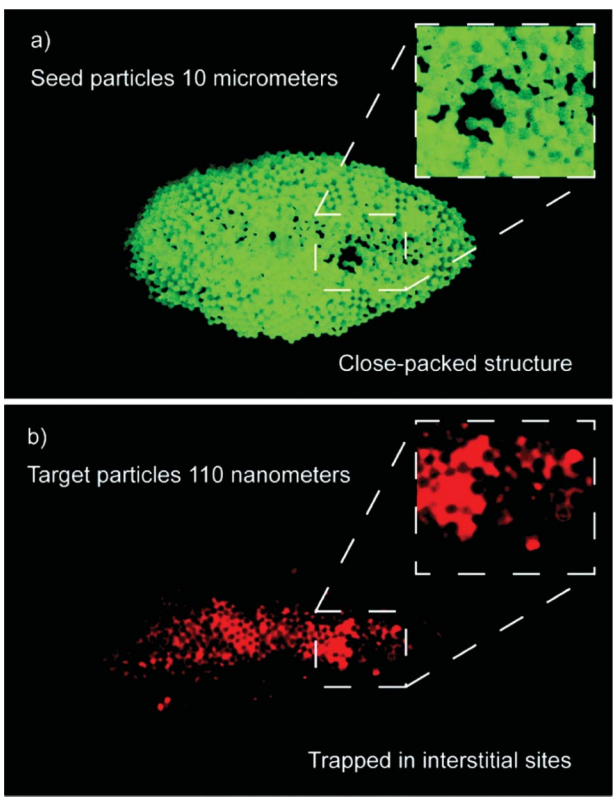

Fig. 8 (a) Seed cluster before nanoparticle capture; 10 μm polystyrene beads. (b) Capture of red fluorescent nanoparticles in the central region of the seed cluster. The inset shows that the nanoparticles are located in the interstitial sites of the close-packed seed cluster.

Inspection of the captured nanoparticles in the seed cluster, Fig. 8, shows that they are located in the interstitial sites of the close packed structure. Some larger packing dislocations were observed in the seed cluster (green) and these can be seen filled out by the captured nanoparticles (red). This suggests that the particles are not only adhering to the surface of the larger beads but form dense clusters of nanoparticles that fill out the interstitial sites in the seed cluster. The captured nanoparticles are also found in the central region of the seed cluster, which could be explained by convective transport by the acoustic streaming (characterized in Fig. 3a). These experiments show that in contrast to other acoustic particle manipulation techniques seed particle aided acoustic trapping allow manipulation of particles at the nanoscale.

Conclusions

This work shows that particle concentration plays a major role in acoustic trapping of sub-micron particles. The reported data demonstrates that increased particle concentrations are required to induce trapping as the particle dimensions are reduced. This is a major obstacle for applications targeting small particles at low concentrations. To alleviate this we demonstrate that the concept of using seed particles to initiate the trapping effects observed at higher concentrations greatly improves this situation and allows capture of sub-micron particles below the established concentration limitations. Using the seed particle strategy, we also demonstrate a 95% trapping efficiency of low abundant bacteria at a continuous flow of 10 uL min^{-1}. The seed particle method scales well with size and allows capture of particles down to the nanometer scale as demonstrated for 110 nm particles. In enrichment applications for pathogen detection the ability to affect 100 nm particles gives the potential for trapping of bacteria and viruses, which is a topic for continued work. Even though the seed particles allow capture of particles at the nanoscale it is probable that the acoustic streaming is very important for translating the particles to the trapping region. Bringing the particles to the trapping site in a controlled manner is anticipated to be a deciding factor when optimizing the capture efficiency in future systems.

Acknowledgements

The authors would like to acknowledge the support from: The Swedish Research Council (Dnr. 621-2010-4389), Vinnova (Innovations for future health-CellCARE), The Crafoord Foundation, The Royal Physiographic Society and Knut & Alice Wallenberg Foundation. These organizations are greatly acknowledged for their financial support.

References

1 J. Nilsson, M. Evander, B. Hammarstrom and T. Laurell, *Anal. Chim. Acta*, 2009, **649**, 141–157.
2 J. Voldman, *Annu. Rev. Biomed. Eng.*, 2006, **8**, 425–454.
3 D. G. Grier, *Nature*, 2003, **424**, 810–816.

4 S. M. Kim, S. H. Lee and K. Y. Suh, *Lab Chip*, 2008, **8**, 1015–1023.
5 A. Ashkin and J. M. Dziedzic, *Science*, 1987, **235**, 1517–1520.
6 M. P. Hughes and H. Morgan, *J. Phys. D: Appl. Phys.*, 1998, **31**, 2205–2210.
7 B. H. Lapizco-Encinas, B. A. Simmons, E. B. Cummings and Y. Fintschenko, *Anal. Chem.*, 2004, **76**, 1571–1579.
8 M. Evander, L. Johansson, T. Lilliehorn, J. Piskur, M. Lindvall, S. Johansson, M. Almqvist, T. Laurell and J. Nilsson, *Anal. Chem.*, 2007, **79**, 2984–2991.
9 B. Vanherberghen, O. Manneberg, A. Christakou, T. Frisk, M. Ohlin, H. M. Hertz, B. Onfelt and M. Wiklund, *Lab Chip*, 2010, **10**, 2727–2732.
10 M. A. Sobanski, C. R. Tucker, N. E. Thomas and W. T. Coakley, *Bioseparation*, 2000, **9**, 351–357.
11 M. S. Limaye, J. J. Hawkes and W. T. Coakley, *J. Microbiol. Methods*, 1996, **27**, 211–220.
12 L. A. Kuznetsova, S. P. Martin and W. T. Coakley, *Biosens. Bioelectron.*, 2005, **21**, 940–948.
13 M. Evander, L. Johansson, T. Lilliehorn, J. Piskur, M. Lindvall, S. Johansson, M. Almqvist, T. Laurell and J. Nilsson, *Anal. Chem.*, 2007, **79**, 2984–2991.
14 J. Hultstrom, O. Manneberg, K. Dopf, H. M. Hertz, H. Brismar and M. Wiklund, *Ultrasound Med. Biol.*, 2007, **33**, 145–151.
15 J. V. Norris, M. Evander, K. M. Horsman-Hall, J. Nilsson, T. Laurell and J. P. Landers, *Anal. Chem.*, 2009, **81**, 6089–6095.
16 O. Manneberg, B. Vanherberghen, J. Svennebring, H. M. Hertz, B. Onfelt and M. Wiklund, *Appl. Phys. Lett.*, 2008, **93**(6), 063901.
17 D. Bazou, L. A. Kuznetsova and W. T. Coakley, *Ultrasound Med. Biol.*, 2005, **31**, 423–430.
18 T. Lilliehorn, U. Simu, M. Nilsson, M. Almqvist, T. Stepinski, T. Laurell, J. Nilsson and S. Johansson, *Ultrasonics*, 2005, **43**, 293–303.
19 B. Hammarstrom, M. Evander, H. Barbeau, M. Bruzelius, J. Larsson, T. Laurell and J. Nilsson, *Lab Chip*, 2010, **10**, 2251.
20 R. Barnkob, P. Augustsson, T. Laurell, H. Bruus, *14th International Conference on Miniaturized Systems for Life Sciences*, 2010, Groningen, The Netherlands, 1247–1249.
21 B. Hammarstrom, T. Laurell and J. Nilsson, *15th International Conference on Miniaturized Systems for Life Sciences*, 2011, Seattle, USA, 1707–1709.
22 S. M. Woodside, B. D. Bowen and J. M. Piret, *AIChE J.*, 1997, **43**, 1727–1736.
23 L. P. Gorkov, *Dokl. Akad. Nauk SSSR*, 1961, **140**, 88.
24 G. Whitworth, M. A. Grundy and W. T. Coakley, *Ultrasonics*, 1991, **29**, 439–444.
25 L. A. Crum, *J. Acoust. Soc. Am.*, 1975, **57**, 1363–1370.
26 M. A. H. Weiser, R. E. Apfel and E. A. Neppiras, *Acustica*, 1984, **56**, 114–119.
27 M. Groschl, *Acustica*, 1998, **84**, 432–447.
28 C. Eckart, *Phys. Rev.*, 1948, **73**, 68–76.
29 L. Rayleigh, *Philos. Trans. R. Soc. London*, 1884, **175**, 1–21.
30 H. Schlichting, *Phys. Z.*, 1932, **33**, 327–335.
31 D. Bazou, W. T. Coakley, K. M. Meek, M. Yang and D. T. Pham, *Colloids Surf., A*, 2004, **243**, 97–104.
32 V. Vivek and K. Eun Sokin *Micro Electro Mechanical Systems, 2000. MEMS 2000. The Thirteenth Annual International Conference on*, 2000, pp. 668-673.
33 C. A. Miles, M. J. Morley, W. R. Hudson and B. M. Mackey, *J. Appl. Microbiol.*, 1995, **78**, 47–54.
34 C. Mikkelsen and H. Bruus, *Lab Chip*, 2005, **5**, 1293–1297.
35 A. Lenshof, C. Magnusson and T. Laurell, *Lab Chip*, 2012, **12**, 1210–1223.